Nonlinear Dyn (2015) 82:1989–2000
DOI 10.1007/s11071-015-2293-9

ORIGINAL PAPER

The influence of tangential and torsional vibrations on the stability lobes in metal cutting

Andreas Otto · **Günter Radons**

Received: 9 March 2015 / Accepted: 20 July 2015 / Published online: 30 July 2015

Abstract Chatter vibrations in machining are studied. Special attention is paid to the effect of structural vibrations in the cutting speed direction. These so-called tangential vibrations may dominate the dynamics in drilling, sawing or grinding, where the torsional dynamic stiffness is much lower than the lateral, axial or radial dynamic stiffness. The inclusion of tangential vibrations in the chip thickness model leads to a delay differential equation (DDE) with state-dependent delay in the time domain. It is shown that the system is equivalent to a DDE with constant delay if it is described in terms of the spindle rotation angle. The analysis of metal cutting vibrations in the angular domain is very useful because in this case the delay is a constant parameter. Numerical examples for turning and drilling processes are presented. An extension of the universal oriented transfer function method for the stability analysis in the frequency domain is presented, which includes the tangential regenerative effect. An additional term appears in the oriented transfer function, which can stabilize or destabilize critical eigenmodes and may also lead to new instabilities in comparison with the conventional analysis.

Keywords Turning · Drilling · Chatter · State-dependent delay · Spindle speed variation

A. Otto (✉) · G. Radons
Institute of Physics, Chemnitz University of Technology, 09107 Chemnitz, Germany
e-mail: andreas.otto@physik.tu-chemnitz.de

1 Introduction

The productivity and efficiency of machine tools are often limited by chatter. Chatter vibrations in metal cutting are large amplitude vibrations between the workpiece and the tool tip. Chatter leads to noise, increased tool wear, bad surface finish and damage of machine tool components. The numerical simulation of machine tool vibrations can be a useful tool for process planning or during the design stage of machine tools. Especially, the stability lobe diagram is used to find chatter-free cutting conditions and to optimize the productivity of machine tools. The stability lobes separate the stable and unstable zones of the self-excited vibrations in the processes.

Since more than 50 years, the regenerative effect is known to be the main reason for self-excited vibrations in metal cutting [8,22]. The regenerative effect is characterized by the influence of delayed structural vibrations at the previous cut on the cutting force and the vibrations at the present cut. Chatter occurs if the closed loop for these self-excited oscillations becomes unstable. Methods for the identification of the stability lobes are described, for example, in [1–3,18]. The time delay as the time between two subsequent cuts tends to be a sensitive parameter with respect to the stability of the process. Recently, the effects of time-varying delays on the stability lobes due to a desired spindle speed variation (SSV) are studied for turning [17], milling [27] and grinding [5].

The influence of tangential vibrations on the stability of metal cutting processes was already studied in [4]. Here, tangential vibrations are structural vibrations parallel to the cutting speed direction, which may occur due to torsion. If the cutting force increases for decreasing cutting velocity, the cutting force can be interpreted as a negative viscous damping term, and self-induced tangential vibrations may appear. Later, the tangential regenerative effect (TRE) was identified in circular sawing processes [14,26]. Since the feed velocity in metal cutting is typically constant but tangential vibrations lead to variations of the cutting velocity, tangential displacements change the chip thickness. The same effect and its consequence on the time delay were later studied for turning [12], milling [6] and drilling [15,25] processes. There are also indications that tangential vibrations significantly affect the stability of self-excited vibrations in grinding [13].

In this paper, we present a universal method for the description and the analysis of the effect of tangential vibrations on the metal cutting dynamics. In Sec. 2, we derive a universal extended chip thickness model for metal cutting processes. Whereas in conventional models the time delay is assumed to be an invariant parameter, in our extended model the time delay is a dynamic variable. With the proposed extended chip thickness model also the mechanism of the TRE, which was initially identified in [14,26], becomes clear. Further, it is known that tangential vibrations lead to a state-dependent delay [12]. In Sec. 3, we present a very useful method for the analysis of the state-dependent delay in machining. The crucial point is a description of the system in terms of the spindle rotation angle, which was already proposed in [23] for turning with SSV. In the angular domain, the delay is constant equal to the angular distance between two subsequent cuts. However, the angular domain representation is hardly found in the literature. In Sec. 4, the semidiscretization for DDEs with a variable delay [10] and the semidiscretization for DDEs with periodic coefficients [11] are used to demonstrate the equivalence between the time and the angular domain representation of a turning process with SSV. Moreover, the generalized oriented transfer function approach [18] is used for the systematical stability analysis of a turning and a drilling example in the frequency domain. The TRE leads to an additional term in the oriented transfer function. In comparison with the conventional model, the TRE can stabilize or destabilize existing critical eigenmodes. If the TRE dominates, it is also possible that new critical eigenmodes emerge with chatter frequencies close to eigenfrequencies of the torsional or tangential eigenmodes.

2 Model

2.1 Structural dynamics

For the description of metal cutting dynamics, the behavior of relative structural displacements $\boldsymbol{r}(t)$ between tool tip and workpiece in response to a load $\boldsymbol{F}(t)$ is necessary. The model takes into account lateral x, y, and axial z as well as torsional θ displacements. The load vector $\boldsymbol{F}$ contains the forces F_x, F_y, F_z in Cartesian coordinates and the cutting torque M w.r.t. the spindle axis. In the frequency domain, the structural displacements $\hat{\boldsymbol{r}}(\omega)$ can be described by the frequency response functions (FRFs) $\Phi_{kl}(\omega)$, $k, l \in \{x, y, z, \theta\}$ in response to the excitation $\hat{\boldsymbol{F}}(\omega)$ [16]. Here, $\hat{\boldsymbol{u}}(\omega)$ denotes the Fourier transform of a vector $\boldsymbol{u}(t)$. Thus, the structural dynamics can be described by

$$\hat{\boldsymbol{r}}(\omega) = \boldsymbol{\Phi}(\omega)\hat{\boldsymbol{F}}(\omega), \tag{1a}$$

or componentwise by

$$\begin{pmatrix} \hat{x} \\ \hat{y} \\ \hat{z} \\ \hat{\theta} \end{pmatrix} = \begin{pmatrix} \Phi_{xx} & \Phi_{xy} & \Phi_{xz} & \Phi_{x\theta} \\ \Phi_{yx} & \Phi_{yy} & \Phi_{yz} & \Phi_{y\theta} \\ \Phi_{zx} & \Phi_{zy} & \Phi_{zz} & \Phi_{z\theta} \\ \Phi_{\theta x} & \Phi_{\theta y} & \Phi_{\theta z} & \Phi_{\theta\theta} \end{pmatrix} \begin{pmatrix} \hat{F}_x \\ \hat{F}_y \\ \hat{F}_z \\ \hat{M} \end{pmatrix}. \tag{1b}$$

In particular, the FRF $\Phi_{kl}(\omega)$ characterizes the behavior of the kth component of the displacements between tool tip and workpiece in response to a harmonic excitation of the lth component of the load on the structure with frequency ω.

2.2 Cutting force

Conversely to the structural model, the cutting force model describes changes of the load in dependence of structural vibrations. Two assumptions are necessary for a noticeable effect of torsional or tangential vibrations on the stability of the cutting process. Firstly, a variation of the chip thickness $h(t)$ leads to a significant variation of the cutting force. And secondly, the cutting force has a nonzero component in tangential direction, i.e., the tangential or torsional eigenmodes are excited by the process. Both assumption are fulfilled in typical cutting processes. Here, we consider a simplified

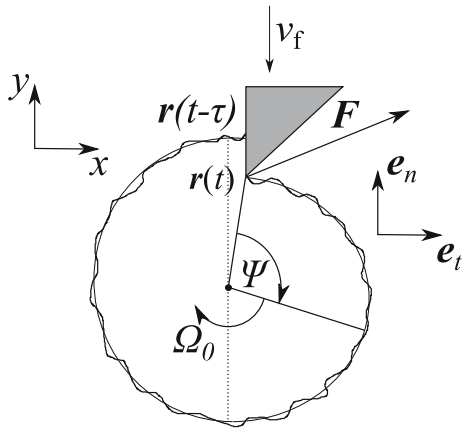

Fig. 1 Geometry of a turning process with vibrations of the tool at the present $\boldsymbol{r}(t)$ and the previous $\boldsymbol{r}(t-\tau)$ cut in normal $\boldsymbol{e}_\mathrm{n}$ and tangential $\boldsymbol{e}_\mathrm{t}$ direction. The kinematics can be described by the workpiece rotation with spindle speed Ω_0 and the feed in negative y-direction with velocity v_f

turning process to demonstrate the typical form of the cutting force model. The geometry and the kinematics of the process are illustrated in Fig. 1. The cutting force $\boldsymbol{F}_\mathrm{tn}(t)$ on the tool tip is composed of a tangential component F_t and a normal component F_n, parallel $\boldsymbol{e}_\mathrm{t}$ and perpendicular $\boldsymbol{e}_\mathrm{n}$ to the cutting speed direction, respectively. For convenience, we choose a linear model and assume that the effect of process damping is negligible,

$$\boldsymbol{F}_\mathrm{tn}(t) = \begin{pmatrix} F_\mathrm{t}(t) \\ F_\mathrm{n}(t) \end{pmatrix} = K_\mathrm{t} \begin{pmatrix} 1 \\ k_\mathrm{n} \end{pmatrix} b h(t). \tag{2}$$

In Eq. (2), K_t is the cutting pressure in tangential direction, k_n is the ratio of normal to tangential cutting pressure, and b is the chip width. We refer to [18] for the cutting force modeling in case of more complex processes with a rotating tool, multiple cutting teeth, or a nonlinear cutting force behavior. The cutting force $\boldsymbol{F}_\mathrm{tn}(t)$ in tangential and normal coordinates at the cutting edge can be transformed by the 4×2 matrix $\boldsymbol{T}$ into the load vector $\boldsymbol{F}(t)$ in Cartesian coordinates

$$\boldsymbol{F}(t) = \boldsymbol{T}\boldsymbol{F}_\mathrm{tn}(t), \quad \boldsymbol{T} = \mathrm{col}\,(\boldsymbol{e}_\mathrm{t}, \boldsymbol{e}_\mathrm{n})\,. \tag{3}$$

2.3 Chip thickness

Regenerative displacements in the normal direction $\boldsymbol{e}_\mathrm{n}$ for the analysis of self-excited vibrations in machining were considered since the pioneering work of [8,22]. Not only normal vibrations at the present cut at time t but also normal vibrations at the previous cut at time $t-\tau$ lead to a modification of the chip thickness. In general, the chip thickness $h(t)$ for an arbitrary cutting process can be characterized by

$$h(t) = n(t-\tau) - n(t), \tag{4}$$

where $n(t)$ is the normal coordinate of the tool position at time t, and τ is the time delay between two subsequent cuts. In particular, for the turning example in Fig. 1 the normal position $n(t)$ can be specified by

$$n(t) = n_0 - v_\mathrm{f} t + \boldsymbol{e}_\mathrm{n}^\mathrm{T} \boldsymbol{r}(t), \tag{5}$$

where n_0 is the initial position, v_f is the constant feed velocity, and $^\mathrm{T}$ denotes transposition. If we put Eq. (5) into Eq. (4), we obtain the well-known conventional chip thickness model

$$h(t) = v_\mathrm{f}\tau + \boldsymbol{e}_\mathrm{n}^\mathrm{T}(\boldsymbol{r}(t-\tau) - \boldsymbol{r}(t)). \tag{6}$$

In Eq. (6), the term $\boldsymbol{e}_\mathrm{n}^\mathrm{T}(\boldsymbol{r}(t-\tau) - \boldsymbol{r}(t))$ is often called dynamic chip thickness, because it describes the chip thickness variations due to dynamic displacements. In contrast, the term $v_\mathrm{f}\tau$ is often called static chip thickness because the time delay τ is typically assumed to be a constant parameter. In the following, we present an accurate model for the time delay τ for situations in cutting processes where the assumption of a constant time delay τ is not adequate.

2.4 Time delay

In contrast to displacements into the normal direction, the effect of displacements in tangential direction $\boldsymbol{e}_\mathrm{t}$ on metal cutting vibrations is only rarely studied in the literature. Since tangential vibrations change the cutting speed, they have an influence on the time delay between two subsequent cuts. Thus, the time delay τ is not only a constant parameter but rather a dynamical variable in the system, i.e., $\tau = \tau(t, \boldsymbol{r}_\mathrm{t})$. The vector function $\boldsymbol{r}_\mathrm{t} = \boldsymbol{r}(t-s)$ with $s \in [0, \tau_\mathrm{max}]$ and the maximum delay $\tau_\mathrm{max} \in \mathbb{R}^+$ are assumed to be the state of the system [12]. The dynamic delay, which is also called state-dependent delay, can be defined implicitly by

$$\delta = \Psi(t) - \Psi(t - \tau(t, \boldsymbol{r}_\mathrm{t})), \tag{7}$$

where δ (in rad) is the angle between two subsequent cuts at the same workpiece location. The angular distance δ between two subsequent cuts is a constant parameter equal to 2π or equal to the tooth pitch. The angle $\psi = \Psi(t)$ (in rad) specifies the angle between the tool tip and a reference point on the workpiece, that is, ψ

is the spindle rotation angle (cf. Fig. 1). For constant nominal spindle speeds Ω_0, the spindle rotation angle ψ can be specified by

$$\psi = \Psi(t) = \Psi_0 + \Omega_0 t - \frac{1}{R}\boldsymbol{e}_\mathrm{t}^\mathrm{T}\boldsymbol{r}(t), \tag{8}$$

where Ψ_0 is the initial angle, and R is the radius of the workpiece. Similar to Eq. (5) for the normal position of the tool tip, there is a static and a dynamic part in Eq. (8). We obtain an implicit relation for the time delay by putting Eq. (8) into Eq. (7)

$$R\delta = v_\mathrm{c}\tau(t, \boldsymbol{r}_\mathrm{t}) + \boldsymbol{e}_\mathrm{t}^\mathrm{T}(\boldsymbol{r}(t - \tau(t, \boldsymbol{r}_\mathrm{t})) - \boldsymbol{r}(t)), \tag{9}$$

where $v_\mathrm{c} = \Omega_0 R$ is the nominal cutting velocity. Eqs. (7)–(9) for the tangential direction have the same structure as Eqs. (4)–(6) for the normal direction. However, in Eq. (9) the angular distance δ is a fixed parameter and defines the state-dependent delay $\tau(t, \boldsymbol{r}_\mathrm{t})$. In Eq. (6), the state-dependent delay is used to determine the chip thickness $h(t)$, which is a free dynamic variable.

2.5 Extended chip thickness model

The substitution of the delay in the conventional chip thickness model Eq. (6) by the relationship Eq. (9) leads to the universal extended chip thickness model

$$h(t) = \rho R\delta + \left(\boldsymbol{e}_\mathrm{n}^\mathrm{T} - \rho\boldsymbol{e}_\mathrm{t}^\mathrm{T}\right)(\boldsymbol{r}(t - \tau(t, \boldsymbol{r}_\mathrm{t})) - \boldsymbol{r}(t)). \tag{10}$$

The dimensionless coefficient $\rho = v_\mathrm{f}/v_\mathrm{c}$ specifies chip thickness variations due to tangential displacements. The extended chip thickness model in Eq. (10) can be understood as follows. The first term is the real nominal chip thickness defined by the parameters of the cutting process. The term $\boldsymbol{e}_\mathrm{n}^\mathrm{T}(\boldsymbol{r}(t - \tau(t, \boldsymbol{r}_\mathrm{t})) - \boldsymbol{r}(t))$ describes dynamic chip thickness variations, directly induced by normal displacements of the structure at the previous and the present cut. This is the well-known normal regenerative effect. The third term $\rho\boldsymbol{e}_\mathrm{t}^\mathrm{T}(\boldsymbol{r}(t - \tau(t, \boldsymbol{r}_\mathrm{t})) - \boldsymbol{r}(t))$ converts tangential displacements at the previous and the present cut into variations of the chip thickness due to an extended or shortened feed motion. This term describes the TRE. The strength of the TRE compared to the normal regenerative effect is characterized by the coefficient ρ. In metal cutting, this value is typically very low $\rho < 0.01$. Hence, the TRE is only relevant if tangential vibrations are much larger than normal vibrations.

With the extended chip thickness model, the cutting force can be written as

$$\begin{aligned}\boldsymbol{F}(t) = {} & bK_\mathrm{t}\boldsymbol{T}\begin{pmatrix}1\\ k_\mathrm{n}\end{pmatrix}\rho R\delta \\ & + bK_\mathrm{t}\boldsymbol{B}_\mathrm{c}(\boldsymbol{r}(t - \tau(t, \boldsymbol{r}_\mathrm{t})) - \boldsymbol{r}(t)).\end{aligned} \tag{11}$$

The first term in Eq. (11) is the static cutting force due to the nominal motion of the spindle and tool, and the second term describes the dynamic cutting force due to dynamic displacements into tangential and normal direction. The coefficient matrix $\boldsymbol{B}_\mathrm{c}$ in the extended model is defined as

$$\boldsymbol{B}_\mathrm{c} = \boldsymbol{T}\begin{pmatrix}1\\ k_\mathrm{n}\end{pmatrix}\left(\boldsymbol{e}_\mathrm{n}^\mathrm{T} - \rho\boldsymbol{e}_\mathrm{t}^\mathrm{T}\right). \tag{12}$$

The entries $\{\boldsymbol{B}_\mathrm{c}\}_{kl}$ of the coefficient matrix with $k, l \in \{x, y, z, \theta\}$ are called directional factors. In particular, the directional factor $\{\boldsymbol{B}_\mathrm{c}\}_{kl}$ specifies variations of the kth component of the force vector due to a displacement of the lth component of the structure. For the conventional model, the directional factors for displacements in tangential direction are zero as can be seen, for example, in [18]. In the extended model, additionally the effect of tangential vibrations on the cutting force is taken into account. The TRE is only one consequence of tangential or torsional vibrations. Another important effect is the state dependence of the time delay $\tau(t, \boldsymbol{r}_\mathrm{t})$.

3 State-dependent delay in machining

3.1 State-dependent delay

The implicit definition of the time delay in Eq. (7) yields a time- and state-dependent delay $\tau(t, \boldsymbol{r}_\mathrm{t})$. The state dependence is indicated by $\boldsymbol{r}_\mathrm{t}$. The state of the system $\boldsymbol{r}_\mathrm{t}$ at time t contains all relevant displacements $\boldsymbol{r}(t - s)$ with $s \in [0, \tau_\mathrm{max}]$, which can affect the time delay or the chip thickness at the present time t or in the future. However, a priori it is not possible to determine the upper bound of the delay τ_max, or the maximum size of the state space of the system without knowing the dynamics $\boldsymbol{r}(t)$ at all times. This illustrates one mathematical problem with the analysis of state-dependent delays. The problem of a minimal state-space representation for similar systems is addressed in [24]. There are also other problems in systems with state-dependent delays such as the existence and uniqueness of solutions or the linearization of DDEs with state-dependent delay [6,21]. Moreover, the implicit nature of Eq. (7)

for the definition of the state-dependent delay prevents a straightforward numerical simulation of the system, for example, with a numerical solver such as the MATLAB routine `ddesd` [20]. In the next subsection, a practical and efficient way for the treatment of state-dependent delay in machining is presented.

3.2 Transformation to the angular domain

As can be seen from Eq. (8), the spindle rotation angle ψ can serve as an independent variable of the system. For the transformation from the time to the angular domain, we consider the spindle rotation angle in the general case

$$\psi = \Psi(t) = \Psi_{\mathrm{nom}}(t) - \frac{1}{R}\boldsymbol{e}_{\mathrm{t}}^{\mathrm{T}}\boldsymbol{r}(t). \tag{13}$$

In contrast to Eq. (8), Eq. (13) can deal with an active SSV with the nominal spindle angle $\Psi_{\mathrm{nom}}(t)$, and the nominal spindle speed $\dot{\Psi}_{\mathrm{nom}}(t) = \Omega(t)$. For typical cutting conditions, the spindle speed $\Omega(t)$ is always much higher than the velocity of the tangential vibrations

$$\frac{\mathrm{d}\psi}{\mathrm{d}t} = \Omega(t) - \frac{1}{R}\boldsymbol{e}_{\mathrm{t}}^{\mathrm{T}}\dot{\boldsymbol{r}}(t) > 0. \tag{14}$$

If Eq. (14) holds, the spindle moves always in the same direction, and a one-to-one mapping between time t and spindle rotation angle ψ is possible. We remark that situations in unstable processes are possible, where Eq. (14) is probably not fulfilled. Such an effect was measured, for example, during chatter vibrations in circular sawing [14,26]. The sunray pattern on the surface of a drilling hole due to axial–torsional chatter vibration may also be a result of a drill, which rotates temporarily backwards [1,19]. However, for backward rotation of the spindle the cutting force model breaks down and it is not clear, which kind of waves are left on the surface of the workpiece. The aim of this paper is not the characterization of the highly nonlinear behavior of chatter vibrations but rather the characterization of the dynamics in the neighborhood of ideal cutting conditions. Ideal cutting is characterized by a stationary or periodic steady state of the vibrations $\boldsymbol{r}(t)$. In this case, Eq. (14) holds. Hence, any variable $\boldsymbol{u}$ of the system can be described as a function of time t or as a function of the spindle angle ψ

$$\tilde{\boldsymbol{u}}(\psi) = \tilde{\boldsymbol{u}}(\Psi(t)) = \boldsymbol{u}(t). \tag{15}$$

The inverse $\Psi^{-1}(\psi)$ of the function $\Psi(t)$ specifies the time t for a known spindle angle ψ and is given by

$$t = \Psi^{-1}(\psi) = \Psi_{\mathrm{nom}}^{-1}\left(\psi + \frac{1}{R}\boldsymbol{e}_{\mathrm{t}}^{\mathrm{T}}\tilde{\boldsymbol{r}}(\psi)\right). \tag{16}$$

The function $\Psi_{\mathrm{nom}}^{-1}(\psi)$ is the inverse of the nominal spindle angle $\Psi_{\mathrm{nom}}(t)$ in the absence of dynamic displacements.

The main advantage of the angular domain representation is the constant angle δ between the present and the previous cut. Thus, the delayed argument $t-\tau(t,\boldsymbol{r}_{\mathrm{t}})$ with the time- and state-dependent delay in the time domain is replaced by the delayed argument $\psi - \delta$ with the constant delay δ in the angular domain

$$\boldsymbol{u}(t-\tau(t,\boldsymbol{r}_{\mathrm{t}})) = \tilde{\boldsymbol{u}}(\Psi(t-\tau(t,\boldsymbol{r}_{\mathrm{t}}))) = \tilde{\boldsymbol{u}}(\psi-\delta). \tag{17}$$

This follows immediately from Eq. (15) and the definition of the state-dependent delay in Eq. (7). Thus, the mathematical treatment of the system with time- and state-dependent delay $\tau(t,\boldsymbol{r}_{\mathrm{t}})$ is clear because it is equivalent to a system with constant delay δ. In the angular domain, the state space of the system is a priori well defined, $\tilde{\boldsymbol{r}}_{\psi} = \tilde{\boldsymbol{r}}(\psi - s)$, with $s \in [0,\delta]$. Furthermore, an explicit expression for the state-dependent delay $\tau(t,\boldsymbol{r}_{\mathrm{t}})$ can be given with Eq. (7) and Eq. (16)

$$\tau(t,\boldsymbol{r}_{\mathrm{t}}) = t - \Psi^{-1}\left(\Psi(t) - \delta\right). \tag{18}$$

Equation (18) can be used for the calculation of the state-dependent delay in time domain simulations of the machine tool vibrations. Equation (18) is formally similar to a relation presented in [17] for the calculation of the delay in case of spindle speed variation. However, in contrast to the investigation in [17], the function $\Psi(t)$ depends also on dynamic displacements $\boldsymbol{r}(t)$. This is the reason why the time delay $\tau(t,\boldsymbol{r}_{\mathrm{t}})$ is, in general, not only time-dependent but also state-dependent. If the nominal spindle speed is constant $\dot{\Psi}_{\mathrm{nom}}(t) = \Omega_0$, Eq. (18) simplifies to a rearranged form of Eq. (9).

3.3 Dynamics in the angular domain

Instead of the calculation of the state-dependent delay with Eq. (18) and the analysis of the system in the time domain, the analysis of the complete dynamics in the angular domain is also possible and often useful. In

general, a dynamical system, describing chatter vibrations in machining, can be written in state-space form as

$$\dot{\boldsymbol{u}}(t)=\begin{pmatrix}\dot{\boldsymbol{u}}_1(t)\\ \dot{\boldsymbol{u}}_2(t)\end{pmatrix}=\begin{pmatrix}\boldsymbol{u}_2(t)\\ \boldsymbol{f}(\Psi(t),\boldsymbol{u}(t),\boldsymbol{u}(t-\tau(t,\boldsymbol{u}_{1t}))\end{pmatrix}, \tag{19}$$

with $\boldsymbol{u}_1(t) = \boldsymbol{r}(t)$ and $\boldsymbol{u}_{1t} = \boldsymbol{r}_t$. Equation (19) is a non-autonomous, nonlinear DDE with time- and state-dependent delay. The following analysis does not depend on the specific form of the function $\boldsymbol{f}$. The dynamics of a time delay system, with a variable delay $\tau(t,\boldsymbol{r}_t)$ as defined in Eq. (7) can be always transformed to a system in the angular domain with constant delay δ. Specific examples for the function $\boldsymbol{f}$ can be found in the literature [1,6,10,12,17,19] and in Sec. 4. A relation between the derivatives in the time and the angular domain can be established by using Eq. (14),

$$\dot{\boldsymbol{u}}(t)=\tilde{\boldsymbol{u}}'(\psi)\frac{\mathrm{d}\psi}{\mathrm{d}t}=\tilde{\boldsymbol{u}}'(\psi)\left(\Omega(t)-\frac{1}{R}\boldsymbol{e}_t^{\mathrm{T}}\dot{\boldsymbol{u}}_1(t)\right). \tag{20}$$

With Eq. (17) and Eq. (20), the angular domain representation of the dynamical system (19) is

$$\begin{aligned}\tilde{\boldsymbol{u}}'(\psi)&=\begin{pmatrix}\tilde{\boldsymbol{u}}_1'(\psi)\\ \tilde{\boldsymbol{u}}_2'(\psi)\end{pmatrix}\\ &=C(\psi)\begin{pmatrix}\tilde{\boldsymbol{u}}_2(\psi)\\ \boldsymbol{f}(\psi,\tilde{\boldsymbol{u}}(\psi),\tilde{\boldsymbol{u}}(\psi-\delta))\end{pmatrix},\end{aligned} \tag{21a}$$

where the varying coefficient $C(\psi)$ is given by

$$C(\psi)=\frac{1}{\tilde{\Omega}(\psi)-\frac{1}{R}\boldsymbol{e}_t^{\mathrm{T}}\tilde{\boldsymbol{u}}_2(\psi)}, \tag{21b}$$

and $\tilde{\Omega}(\psi) = \Omega(t)$ is the angular domain representation of the nominal spindle speed. Equation (21a) is a non-autonomous, nonlinear DDE with constant delay δ and equivalent to Eq. (19) unless condition (14) is violated. The time dependence and state dependence of the time delay $\tau(t,\boldsymbol{u}_{1t})$ in Eq. (19) were converted into an additional non-autonomous and nonlinear prefactor in Eq. (21a). The denominator of the prefactor in Eq. (21b) becomes zero if the condition (14) for a bijective mapping between time t and angle ψ is no longer fulfilled. The analytical treatment as well as the numerical analysis of the system in the angular domain with a constant delay δ is more suitable than the analysis of the system in the time domain with a time- and state-dependent delay. The reason is that in the angular domain the minimal state space is constant, and many methods for the analysis of time delay systems are optimized for constant delays.

4 Stability analysis

In this section, the stability analysis of cutting processes with the inclusion of the effect of tangential and torsional vibrations is presented. The displacements and velocities $\boldsymbol{u}(t)$ of the structural vibrations are assumed to be in the form

$$\boldsymbol{u}(t)=\boldsymbol{u}_{\mathrm{s}}(t)+\boldsymbol{u}_{\mathrm{e}}(t). \tag{22}$$

In Eq. (22), $\boldsymbol{u}_{\mathrm{s}}(t)$ is a steady-state solution of the nonlinear DDE Eq. (19). For ideal cutting without chatter vibrations, the steady state is characterized by a constant or periodic function. Perturbations of the ideal cutting solution are specified by $\boldsymbol{u}_{\mathrm{e}}(t)$. For the stability analysis, the asymptotic behavior of the small perturbations $\boldsymbol{u}_{\mathrm{e}}(t)$ around the ideal cutting solution $\boldsymbol{u}_{\mathrm{s}}(t)$ is investigated. The system is stable or unstable, respectively, if the amplitudes of the perturbations $\boldsymbol{u}_{\mathrm{e}}(t)$ decrease or increase with time. In machining, the stability of the ideal cutting solution is typically illustrated via the stability lobe diagram. The stability lobes separate stable and unstable cutting conditions in a parameter plane spanned by nominal spindle speed Ω_0 and chip width b. The identification of the stability lobes for three typical cutting processes with time- or state-dependent delay is shown below.

4.1 Turning with SSV

In this subsection, the comparison of the stability analysis in the time and the angular domain is demonstrated for a turning model with SSV. Here, the influence of tangential or torsional vibrations on the stability is neglected. The structural dynamics can be described by one dominant eigenmode in the normal direction, i.e., the y-direction in Fig. 1, with eigenfrequency ω_{n} and damping ratio ζ. The state variables are the velocities and displacements of the tool tip perturbations in y-direction $\boldsymbol{u}_{\mathrm{e}} = \mathrm{col}\,(\dot{y}_{\mathrm{e}}, y_{\mathrm{e}})$. In state-space representation, the dynamics around the steady-state solution $\boldsymbol{u}_{\mathrm{s}}$ can be described by [10]

$$\begin{aligned}&\dot{\boldsymbol{u}}_{\mathrm{e}}(t)=\boldsymbol{A}\boldsymbol{u}_{\mathrm{e}}(t)+\boldsymbol{B}\boldsymbol{u}_{\mathrm{e}}(t-\tau(t)),\\ &\boldsymbol{A}=\begin{pmatrix}0 & 1\\ -\omega_{\mathrm{n}}^2(1+w) & -2\zeta\omega_{\mathrm{n}}\end{pmatrix},\quad \boldsymbol{B}=\begin{pmatrix}0 & 0\\ \omega_{\mathrm{n}}^2 w & 0\end{pmatrix}.\end{aligned} \tag{23}$$

The dimensionless chip width w is proportional to the real chip width b and the cutting force coefficient K_{t}.

The exact relationship between w and b also depends on the orientation, the modal mass and the eigenfrequency of the considered eigenmode of the structure. The time-varying delay $\tau(t)$ is specified by Eq. (18) with $\Psi(t) = \Psi_{\text{nom}}(t)$. The equivalent description of the system in the angular domain according to Eq. (21a) is

$$\tilde{\boldsymbol{u}}'_{\text{e}}(\psi) = \frac{1}{\tilde{\Omega}(\psi)} \left(\boldsymbol{A}\tilde{\boldsymbol{u}}_{\text{e}}(\psi) + \boldsymbol{B}\tilde{\boldsymbol{u}}_{\text{e}}(\psi - \delta) \right). \tag{24}$$

The time-varying delay $\tau(t)$ in Eq. (23) was converted into a time-varying denominator $\tilde{\Omega}(\psi) = \Omega(\Psi_{\text{nom}}^{-1}(t))$ in Eq. (24). The stability analysis of turning with SSV in the angular domain representation with a constant angular delay $\delta = 2\pi$ was already shown in [23]. However, Tsao et al. have chosen a sinusoidal $\tilde{\Omega}(\psi)$, i.e., a sinusoidal SSV in the angular domain, which is not the generic case for an application. Furthermore, they have not compared their results with the results for the equivalent system in the time domain.

In this example, a sinusoidal SSV in the time domain $\Omega(t) = \Omega_0(1 + R_A \cos(2\pi \nu_m t))$ is chosen, where $R_A = 0.15$ is the relative amplitude and $\nu_m = 1$ Hz the frequency of the spindle speed modulation. The parameters for the structural dynamics are selected to be $\omega_{\text{n}} = 2\pi\, 100$ Hz and $\zeta = 0.03$. Two types of the semi-discretization method were applied for the calculation of the stability lobes. On the one hand, the semidiscretization for a time-varying delay [10] was used for the stability analysis of Eq. (23) in the time domain. On the other hand, the semidiscretization for time-varying coefficients [11] was used for the analysis of Eq. (24) in the angular domain. The results are shown in Fig. 2 and coincide very well.

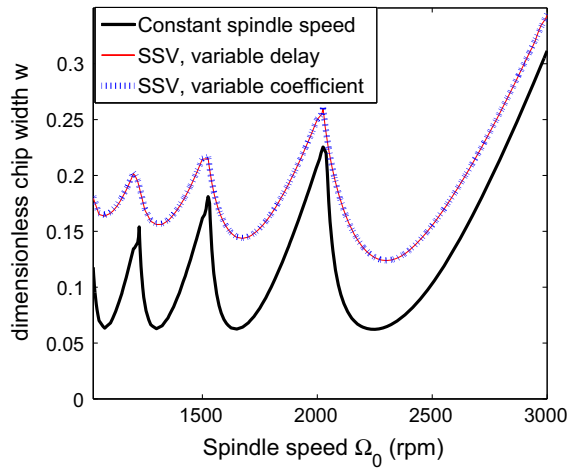

Fig. 2 Comparison of the stability lobes for turning with SSV from Eq. (23) in the time domain (*red*, *solid*) and Eq. (24) in the angular domain (*blue*, *dashed*). The results coincide as required. The stability lobes for constant spindle speed (*black*, *thick*) are also shown. (Color figure online)

4.2 Turning with tangential vibrations

Now, a turning process with constant nominal spindle speed Ω_0 is investigated, which includes the effect of tangential vibrations on the dynamics. The structure is assumed to be flexible into tangential and normal direction and rigid in axial and torsional direction. In this case, the matrix $\boldsymbol{T}$ is the two-dimensional identity matrix because the tangential and normal direction coincide with the x- and $y-$direction (see Fig. 1). The cutting force for such a process was already derived in Sec. 2. With Eq. (11) and Eq. (12), the load on the structure can be written as

$$\begin{aligned}\boldsymbol{F}(t) = \begin{pmatrix} F_x(t) \\ F_y(t) \end{pmatrix} &= bK_{\text{t}} \begin{pmatrix} 1 \\ k_{\text{n}} \end{pmatrix} \rho R \delta \\ &+ bK_{\text{t}} \begin{pmatrix} -\rho & 1 \\ -\rho k_{\text{n}} & k_{\text{n}} \end{pmatrix} \left(\boldsymbol{r}(t - \tau(t, \boldsymbol{r}_{\text{t}})) - \boldsymbol{r}(t) \right).\end{aligned} \tag{25}$$

In this turning process, ideal cutting is characterized by an excitation of the structure with the static part of the cutting force without dynamic displacements. This static excitation during the process leads to a static displacement $\boldsymbol{r}_{\text{s}}(t) = \boldsymbol{r}^*$. Since the structural behavior is assumed to be linear, the state-dependent delay $\tau(t, \boldsymbol{r}_{\text{t}})$ in the dynamic part of the cutting force is the only nonlinearity of the system. Thus, the linearization can be done by the determination of the time delay $\tau(t, \boldsymbol{r}_{\text{t}}) = \tau_{\text{s}}(t, \boldsymbol{r}^*)$ for the ideal cutting solution with Eq. (9). In particular, for the static displacement $\boldsymbol{r}^*$ the time delay is a constant delay $\tau_{\text{s}}(t, \boldsymbol{r}^*) = \tau^* = \delta \Omega_0^{-1}$.

The behavior of the perturbations $\boldsymbol{r}_{\text{e}}(t)$ around the ideal cutting solution can be described with the structural behavior Eq. (1a) and the dynamic part of the cutting force Eq. (25) with $\tau(t, \boldsymbol{r}_{\text{t}}) = \tau^*$. Directly at the stability border the perturbations $\boldsymbol{r}_{\text{e}}(t)$ are periodic oscillations with the chatter frequency ω_{c} and constant amplitudes. The following eigenvalue equation holds for the frequency domain representation of the periodic perturbations $\boldsymbol{r}_{\text{e}}(t)$ at the stability border

$$\begin{pmatrix}\hat{x}_\mathrm{e}\\ \hat{y}_\mathrm{e}\end{pmatrix} = bK_\mathrm{t}\begin{pmatrix}\Phi_{xx} & \Phi_{xy}\\ \Phi_{yx} & \Phi_{yy}\end{pmatrix}\begin{pmatrix}-\rho & 1\\ -\rho k_\mathrm{n} & k_\mathrm{n}\end{pmatrix} \times \left(\mathrm{e}^{-i\omega\tau^*}-1\right)\begin{pmatrix}\hat{x}_\mathrm{e}\\ \hat{y}_\mathrm{e}\end{pmatrix}. \tag{26}$$

Following [18], the oriented transfer function $\sigma(\omega)$ which is the nonzero eigenvalue of the matrix product $\boldsymbol{\Phi}(\omega)\boldsymbol{B}_\mathrm{c}$ is given by

$$\sigma(\omega) = k_\mathrm{n}\Phi_{yy}(\omega) + \Phi_{yx}(\omega) - \rho\left(\Phi_{xx}(\omega) + k_\mathrm{n}\Phi_{xy}(\omega)\right). \tag{27}$$

For $\rho = 0$, Eq. (27) is identical to the results in Ref. [18]. The additional term with the TRE coefficient ρ specifies the influence of the TRE on the oriented transfer function. The limiting chip width b_c, which separates stable from unstable cutting conditions, can be calculated by the well-known stability law of Tlusty

$$b_\mathrm{c}(\omega_\mathrm{c}) = -\frac{1}{2K_\mathrm{t}\sigma_r(\omega_\mathrm{c})}. \tag{28}$$

Thus, the negative real part $\sigma_r(\omega)$ of the oriented transfer function determines the stability.

A special case of the influence of tangential vibrations on the stability behavior of turning processes was already studied in [12]. In this paper, cross FRFs were neglected $\Phi_{xy} = \Phi_{yx} = 0$ and an identical structural behavior in x- and y-direction $\Phi_{xx} = \Phi_{yy} = \Phi$ was assumed. In this case, the critical chip width can be calculated by

$$b_\mathrm{c}(\omega) = -\frac{1}{2K_\mathrm{t}\mathrm{Re}(\Phi(\omega))\,(k_\mathrm{n}-\rho)}. \tag{29}$$

Eq. (29) with $\rho = 0$ is the known stability criterion for the conventional turning model [3]. As was already reported in [12], the TRE with $\rho > 0$ is responsible for an increase in the critical chip width b_c by a factor of $k_\mathrm{n}/(k_\mathrm{n}-\rho)$ in comparison with the critical chip width for the conventional model without tangential vibrations. In general, tangential vibrations can also destabilize the system dependent on the behavior of the FRFs in x- and y-direction.

Another special case occurs if the structure is flexible in x-direction but rigid in y-direction, that is, vibrations of the structure do not affect the chip thickness directly. However, due to the TRE the system can become unstable and the critical chip width is given by

$$b_\mathrm{c}(\omega) = \frac{1}{2K_\mathrm{t}\mathrm{Re}(\Phi_{xx}(\omega))\rho}. \tag{30}$$

In this case, the instability is due to vibrations in tangential direction, completely decoupled from the dynamics in the normal direction. This means that the TRE may not only stabilize or destabilize critical eigenmodes in turning but may also lead to the occurence of new instabilities due to critical eigenmodes in the tangential direction. As can be derived from Eq. (30), such instabilities are characterized by chatter frequencies lower than the eigenfrequency of the structure.

For turning processes in the industry at a real lathe, the behavior of the structural dynamics is complex and the general form of the oriented transfer function in Eq. (27) can be used to determine the stability lobes.

4.3 Axial–torsional chatter in drilling

A stability analysis of axial–torsional chatter in drilling was already presented in the literature [1,7,19]. In [7], the TRE was not considered, and in [1,19] the impact of the TRE on the stability lobes was not studied separately. For the purpose of illustration, only axial z and torsional θ vibrations of the tool are considered, which are decoupled from lateral vibrations [19]. The geometry of the process is shown in Fig. 3. The matrix $\boldsymbol{T}$ can be specified by

$$\boldsymbol{T} = \begin{pmatrix}0 & 1\\ R & 0\end{pmatrix}. \tag{31}$$

Here, R is the mean radius of the cutting lips. In the theory, the moment M w.r.t. the drill axis is generated by the product of the radius R and the tangential cutting force F_t, where the tangential cutting force F_t is

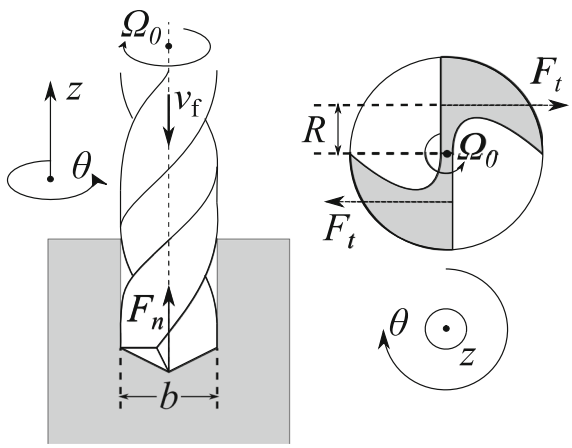

Fig. 3 Geometry of a drilling process with axial z and torsional θ vibrations

Table 1 Parameters for drilling example [19]

Structural dynamics				
Mode index	Frequency ω_n	Damping ζ	Stiffness k	Sign
zz	3358 Hz	2 %	1.06×10^8 N/m	+
$z\theta$	3358 Hz	2 %	4.34×10^5 Nm/m	−
θz	3358 Hz	2 %	4.92×10^5 N/rad	−
$\theta\theta$	3358 Hz	2 %	7.78×10^2 Nm/rad	+
Cutting force				
K_t	k_n	Radius R	Feed per tooth $v_f\tau^*$	ρ
1235 N/mm^2	0.23	6.62 mm	0.4 mm	0.019

interpreted as a point force (see Fig. 3) instead of a force distributed along the cutting edge as in practice. The load vector on the structure for this process can be defined as

$$\boldsymbol{F}(t) = \begin{pmatrix} F_z(t) \\ M(t) \end{pmatrix} = bK_t \begin{pmatrix} k_n \\ R \end{pmatrix} \rho R \delta + bK_t \begin{pmatrix} k_n & -\rho k_n R \\ R & -\rho R^2 \end{pmatrix} (\boldsymbol{r}(t - \tau(t, \boldsymbol{r}_t)) - \boldsymbol{r}(t)). \tag{32}$$

The problem is qualitatively equivalent to the turning example with tangential vibrations as described in the previous subsection. Ideal cutting is characterized by a static displacement $\boldsymbol{r}_s(t) = \boldsymbol{r}^*$, and the linearization is done by replacing the state-dependent delay by the constant delay $\tau^* = \delta\Omega_0^{-1}$. Note that for this process with two cutting lips the angular distance between two subsequent cuts is $\delta = \pi$. The perturbations at the stability lobes can be described in the frequency domain formally similar to Eq. (26). The oriented transfer function $\sigma(\omega)$ for axial–torsional vibrations in drilling, which is the nonzero eigenvalue of the matrix product $\boldsymbol{\Phi}(\omega)\boldsymbol{B}_c$, can be determined by

$$\sigma(\omega) = k_n \Phi_{zz}(\omega) + \Phi_{z\theta}(\omega) R - \rho \left(k_n \Phi_{\theta z}(\omega) R + \Phi_{\theta\theta}(\omega) R^2 \right). \tag{33}$$

For $\rho = 0$, Eq. (33) is similar to the results obtained in [18] and specifies direct modifications of the chip thickness due to normal and tangential forces at the cutting lips. The third term with the TRE coefficient ρ characterizes modifications of the chip thickness due to torsional vibrations of the drill, created by normal and tangential forces at the cutting lips. Again, the critical chip width b_c, that separates stable from unstable cutting conditions, can be calculated with Eq. (28).

The effect of torsional vibrations on the stability of drilling is shown for an example from the literature. The parameters for the structural dynamics, the cutting force and the drill geometry are taken from [19] and are summarized in Table 1. The FRF matrix $\boldsymbol{\Phi}(\omega)$ for axial–torsional vibrations can be determined by

$$\begin{pmatrix} \Phi_{zz} & \Phi_{z\theta} \\ \Phi_{\theta z} & \Phi_{\theta\theta} \end{pmatrix} = \frac{\omega_n^2}{\omega_n^2 - \omega^2 + 2\omega_n \zeta i\omega} \begin{pmatrix} +k_{zz}^{-1} & -k_{z\theta}^{-1} \\ -k_{\theta z}^{-1} & +k_{\theta\theta}^{-1} \end{pmatrix}, \tag{34}$$

with the eigenfrequency ω_n, the damping ratio ζ and the stiffnesses k_{kl}, $k, l \in \{z, \theta\}$ of the axial–torsional mode. In Fig. 4a, the real parts of the FRFs for normal z and tangential displacements θR in response to normal F_z and tangential F_t forces are shown. The direct FRFs Φ_{zz} and $\Phi_{\theta\theta} R^2$ (solid) have a positive real part for frequencies smaller than the eigenfrequency, $\omega < \omega_n$. This is the generic case, where the orientations of displacements and forces are equal, indicated by a positive sign in Table 1. However, the cross FRFs $\Phi_{z\theta} R$ and $\Phi_{\theta z} R$ (dashed) have a negative real part for $\omega < \omega_n$, characterized by a negative sign in Table 1. This means that a tangential force at the tool tip in positive θ-direction leads to a negative z-displacement and vice versa. In other words, the tangential force untwists the twist drill and leads to an increase in the length of the drill.

Figure 4b shows the oriented transfer function $\sigma(\omega)$ according to Eq. (33) for the drilling example without (black, dashed) and with (black, solid) TRE. Furthermore, the dominant term $\Phi_{z\theta} R$ (green/gray, dashed) of $\sigma(\omega)$ is shown. The behavior of $\sigma(\omega)$ is characterized by a negative real part for frequencies $\omega < \omega_n$, which has been already reported in [7]. Even though practically the nominal feed per tooth $v_f\tau^* = 0.4$ mm is

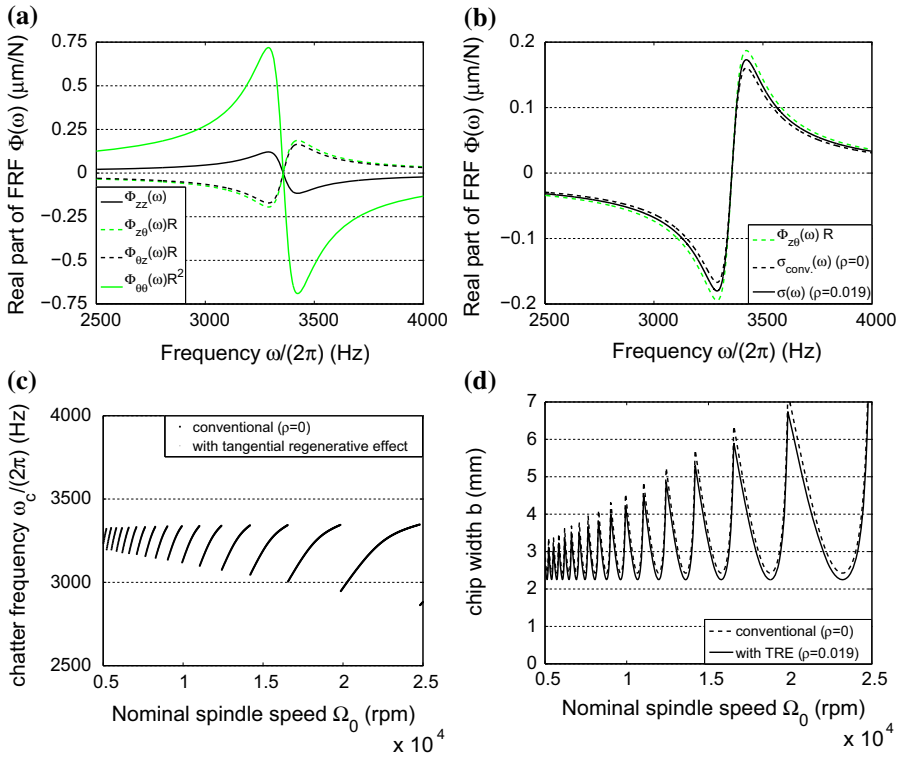

Fig. 4 **a** The magnitude of the tangential direct FRF $\Phi_{\theta\theta} R^2$ dominates the structural behavior, but **b** the oriented transfer function $\sigma(\omega)$ in Eq. (33) is dominated by the cross FRF $\Phi_{z\theta} R$. The change of $\sigma(\omega)$ due to the TRE is small. **c** The TRE does not change the chatter frequencies, but **d** leads to a slight destabilization of the process. (Color figure online)

already set too high for this kind of tool, the strength of the TRE $\rho = 0.019$ is quite small (cf. Table 1). As a result, the effect of torsional vibrations on $\sigma(\omega)$ is small. The chatter frequencies for the process are shown in Fig. 4c. According to Tlusty's law Eq. (28), the negative real part of $\sigma(\omega)$ determines the limiting depth of cut. Thus, the chatter frequencies are smaller than the eigenfrequency $\omega_n = 3358$ Hz of the axial–torsional mode. The TRE does not change the chatter frequencies of the process. This is due to the fact that the chatter frequency ω_c for a specific nominal spindle speed Ω_0 is determined by the phase of the oriented transfer function σ [2]. However, the four relevant FRFs of the axial–torsional eigenmode have the same phase. Only the magnitude differs from each other due to different stiffness parameters in Eq. (34). The stability lobes without (black, dashed) and with (black, solid) TRE are shown in Fig. 4d. Here, the TRE leads to a slight destabilization of the process. This is due to an increased negative minimum of the oriented transfer function of the extended model with TRE compared to the conventional model (cf. Fig. 4b), which can be explained by the signs of the FRFs in Eq. (33) and the signs of the stiffnesses in Eq. (34).

5 Conclusion

The effect of torsional and tangential vibrations on metal cutting dynamics was investigated. Applications are turning, boring, milling, drilling or sawing processes, where vibrations of the tool or the workpiece parallel to the cutting speed direction are much larger than vibrations perpendicular to it. Apart from the conventional dynamic chip thickness variation due to normal vibrations, vibrations in cutting speed direction lead to an additional dynamic variation of the chip thickness. We derived a universal extended chip thickness model, which includes the so-called TRE on the chip thickness. Furthermore, tangential vibrations lead to a state-dependent delay. We have shown that the dynamics of metal cutting vibrations can be also described in terms of the covered spindle rotation angle instead of time. This angular domain representation can be either used to calculate the state-dependent delay for the time domain model or the complete model can be converted to the angular domain. The main advantage of the angular domain representation is that the delay in the system is always constant and equal to the tooth pitch.

We have analyzed the stability of turning and drilling processes. In this case, the ideal stable cutting process is characterized by constant displacements and a constant delay. In this case, the identification of the stability lobes in the frequency domain is suitable. We have shown that the TRE leads to an additional term in the oriented transfer function in comparison with the conventional model. The TRE can stabilize or destabilize the process. Further, we have demonstrated that a new instability due to the TRE is possible, which solely occurs due to tangential or torsional vibrations. Such instabilities are known from circular sawing process [26] and may be also relevant in deep hole drilling, where the compliance in torsional direction is much lower than in the other directions [9]. If stable cutting is characterized by a periodic delay, the analysis of the system in the angular domain with a constant angular delay is more advantageous than the analysis in the time domain. We have illustrated the equivalence between the time and the angular domain representation by an example of turning with spindle speed variation.

Acknowledgments We thank Dr. Josef Kleckner for helpful discussions.

Compliance with ethical standards

Conflicts of interest The authors gratefully acknowledge the financial support of the German Federal Ministry of Education and Research (BMBF) in the research and development project ReffiZ within the Framework Concept "Research for Tomorrow's Production" (Fund Number 02PC1010) and managed by the Project Management Agency Forschungszentrum Karlsruhe (PTKA).

References

1. Ahmadi, K., Altintas, Y.: Stability of lateral, torsional and axial vibrations in drilling. Int. J. Mach. Tools Manuf. **68**, 63–74 (2013)
2. Altintas, Y.: Manufacturing Automation: Metal Cutting Mechanics, Machine Tool Vibrations, and CNC Design. Cambridge University Press, New York (2000)
3. Altintas, Y., Weck, M.: Chatter stability of metal cutting and grinding. CIRP Ann. **53**, 619–642 (2004)
4. Arnold, R.: The mechanism of tool vibration in the cutting of steel. Proc. Inst. Mech. Eng. **154**(1), 261–284 (1946)
5. Álvarez, J., Barrenetxea, D., Marquínez, J., Bediaga, I., Gallego, I.: Effectiveness of continuous workpiece speed variation (cwsv) for chatter avoidance in throughfeed centerless grinding. Int. J. Mach. Tools Manuf. **51**(12), 911–917 (2011)
6. Bachrathy, D., Stépán, G., Turi, J.: State dependent regenerative effect in milling processes. J. Comput. Nonlinear Dyn. **6**(4), 041,002 (2011)
7. Bayly, P., Metzler, S., Schaut, A., Young, K.: Theory of torsional chatter in twist drills: model, stability analysis and composition to test. J. Manuf. Sci. Eng. **123**(4), 552–561 (2002)
8. Danek, O., Polacek, M., Spacek, J., Tlusty, J.: Selbsterregte Schwingungen an Werkzeugmaschinen. VEB Technik Berlin, Berlin (1962)
9. Haag, F., Kleckner, J., Schöpf, J.: Structural dynamics characterization of a deep-hole drill through modal analysis including torsional modes. In: Proceedings of the 13th Euspen International Conference, Berlin, Germany, pp. 145–148 (2013)
10. Insperger, T., Stépán, G.: Stability analysis of turning with periodic spindle speed modulation via semi-discretization. J. Vib. Control **10**(12), 1835–1855 (2004)
11. Insperger, T., Stépán, G.: Updated semi-discretization method for periodic delay-differential equations with discrete delay. Int. J. Numer. Meth. Eng. **61**, 117–141 (2004)
12. Insperger, T., Stépán, G., Turi, J.: State-dependent delay in regenerative turning processes. Nonlin. Dyn. **47**, 275–283 (2007)
13. Mannan, M., Drew, S., Stone, B., Wager, J.: Torsional vibration effects in grinding? CIRP Ann. **49**(1), 249–252 (2000)
14. Milberg, J., Reinhart, G., Zaeh, M.F.: Model-aided adaptive control constraint on circular sawing machines. Ann. WGP **2**(1), 117–122 (1994)
15. Nandakumar, K., Wiercigroch, M.: Stability analysis of a state dependent delayed, coupled two DOF model of drillstringvibration. J. Sound Vib. **332**(10), 2575–2592 (2013)
16. Otto, A., Khasawneh, F.A., Radons, G.: Position-dependent stability analysis of turning with tool and workpiece compliance. Int. J. Adv. Manuf. Technol. **79**(9), 1453–1463 (2015)
17. Otto, A., Radons, G.: Application of spindle speed variation for chatter suppression in turning. CIRP J. Manuf. Sci. Technol. **6**(2), 102–109 (2013)
18. Otto, A., Rauh, S., Kolouch, M., Radons, G.: Extension of Tlusty's law for the identification of chatter stability lobes in multi-dimensional cutting processes. Int. J. Mach. Tools Manuf. **82–83**, 50–58 (2014)
19. Roukema, J., Altintas, Y.: Generalized modeling of drilling vibrations. part i: time domain model of drilling kinematics, dynamics and hole formation. Int. J. Mach. Tools Manuf. **47**(9), 1455–1473 (2007)
20. Shampine, L.: Solving odes and ddes with residual control. Appl. Num. Math. **52**(1), 113–127 (2005)
21. Sieber, J.: Finding periodic orbits in state-dependent delay differential equations as roots of algebraic equations. Discrete Contin. Dyn. Syst. **32**(8), 2607–2651 (2012)
22. Tobias, S.A.: Schwingungen an Werkzeugmaschinen. Hanser, München (1961)
23. Tsao, T., McCarthy, M., Kapoor, S.: A new approach to stability analysis of variable speed machining systems. Int. J. Mach. Tools Manuf. **33**(6), 791–808 (1993)
24. Verriest, E.: Causal behavior of switched delay systems as multi-mode multi-dimensional systems. In: Proceedings of the 8th IFAC Workshop on Time-Delay Systems, Criaova, Romania, pp. 414–419 (2009)

25. Voronov, S., Gouskov, A., Kvashnin, A., Butcher, E., Sinha, S.: Influence of torsional motion on the axial vibrations of a drilling tool. J. Comput. Nonlinear Dyn. **2**(1), 58–64 (2007)
26. Zaeh, M.F.: A new instability mechanism in milling and circular sawing operations and simulation in the time and frequency domain. In: Proceedings of the 19th ISMA, Leuven, Belgium, pp. 1091–1102 (1994)
27. Zatarain, M., Bediaga, I., Muñoa, J., Lizarralde, R.: Stability of milling processes with continuous spindle speed variation: analysis in the frequency and time domains, and experimental correlation. CIRP Ann. **57**(1), 379–384 (2008)